Applied Thermal Engineering 231 (2023) 120876

Contents lists available at ScienceDirect

Applied Thermal Engineering

journal homepage: www.elsevier.com/locate/ate

Research Paper

Effect of fill length and distribution system on the thermal performance of an inverted cooling tower

P. Navarro [a], J. Ruiz [b,*], A.S. Kaiser [a], M. Lucas [b]

[a] Departamento de Ingeniería Térmica y de Fluidos, Universidad Politécnica de Cartagena, Dr. Fleming, s/n, 30202 Cartagena, Spain
[b] Departamento de Ingeniería Mecánica y Energía, Universidad Miguel Hernández, Avda. de la Universidad, s/n, 03202 Elche, Spain

ARTICLE INFO

Keywords:
Cooling tower
Thermal performance
Spray configuration
Nozzle arrangement

ABSTRACT

In the design of a cooling tower there are two key aspects, the thermal performance and emissions level. The main objective of this paper was the experimental optimisation in terms of thermal performance of a new prototype of the forced, mechanical-draft, wet, inverted cooling tower. In this sense, the fill length and the nozzle arrangement (position and hydraulic characteristics) have been investigated. The novelty of the work is that the cooling tower studied has practically zero levels of emission of particles (0.00015% of circulating water). The results indicate that the upper manifold (only parallel flow) presents 24 % better results than the intermediate manifold (mixed and parallel flow mixture) and 37 % better than the lower manifold (equal to the intermediate but with greater distance to the fan). Moreover, the fill has influence on all manifolds operation, since in all manifolds much of the cooling takes place in the parallel flow arrangement. The performance for the 1.6 m fill length is 27% better than for the other two lengths tested. So the combination of a more uniform flow and a larger surface area of exchange will result, in the light of the results obtained, in the best configuration.

1. Introduction

The operation principle of water-cooled systems, such as cooling towers, involves direct contact between two fluid streams of warm water and unsaturated air. Apart from the heat transfer due to temperature difference, mass transfer occurs between liquid and gas phases also due to the vapour concentration difference between them. As a consequence, water evaporates and cools down, while the air moistens and becomes warmer.

Drift emissions, which refer to water droplets that are not evaporated during the cooling process and are carried away by the air stream into the atmosphere, have been widely studied as a potential hazard in cooling towers [1–4]. However, the major concern regarding drift emissions is their impact on human health. Harmful pathogens, such as Legionella pneumophila, can be present in the tower basin due to inadequate maintenance [5] and can be released into the atmosphere as aerosols from cooling towers. Inhaling these airborne particles can lead to the development of Legionnaires' disease, a well-known respiratory illness.

A new prototype, conceived to minimise the environmental impact of a cooling tower, was presented and analysed in Ruiz et al. [6]. This novel design was termed by the authors as the inverted cooling tower (Fig. 1(a)) and its main purpose was to prevent the dispersion of water droplets into the atmosphere during its operation. The results obtained by the authors revealed that the purpose by which the inverted tower was created had been achieved, since nearly-zero emission levels were observed during the experiments. They reported drift values of 0.00015% of the circulating water, which is significantly lower than the limits set by international standards, such as Royal Decree RD 487/2022 [7] in Spain (0.002%) and Australian standard AS/NZS 3666 [8] (0.02%). However, the results showed that further improvements could still be made in the thermal performance. A comparative study was conducted and it was found that the inverted cooling tower was outperformed by a commercial tower of similar characteristics, [9]. The observed differences where up to 41.16%. This fact constituted the main motivation of this research.

The thermal performance of a wet cooling tower is mainly affected by the design and operation of its components, such as the fill, the water distribution system or the drift eliminator, [10,11].

Several studies addressing the influence of the fill on the cooling tower thermal performance can be found in the literature. In Mirabdolah et al. [12], the use of different rotational splash type fills in a forced draft counterflow wet cooling tower was experimentally studied. The results showed that the speed of rotation of the fill significantly improved the characteristic of the tower. Gao et al. [13] and Zhou

* Corresponding author.
E-mail address: j.ruiz@umh.es (J. Ruiz).

https://doi.org/10.1016/j.applthermaleng.2023.120876
Received 10 February 2023; Received in revised form 3 May 2023; Accepted 28 May 2023
Available online 1 June 2023

Nomenclature

A	frontal area (m^2)
a_V	surface area of exchange per unit of volume (m^{-2} m^3)
c_p	specific heat (J kg^{-1} K^{-1})
f	frequency level of the fan (Hz)
h	enthalpy (J kg^{-1})
h_C	heat transfer coefficient (W m^{-2} K^{-1})
h_D	mass transfer coefficient (kg m^{-2} s^{-1})
h_v	enthalpy of vaporisation (J kg^{-1})
Le	Lewis number ($= h_c/\left(h_d c_{p_m}\right)$)
L_f	fill length (m)
$\dot{m}$	mass flow rate (kg s^{-1})
Me	Merkel number ($= h_D a_V V/\dot{m}_w$)
$\dot{m}_s$	Mass flow exiting the cooling tower (kg s^{-1})
$\dot{m}_w$	Mass flow sprayed by the cooling tower (kg s^{-1})
p	pressure (Pa)
Q	total heat transferred from water to air (W)
Q_c	convective heat transferred from water to air (W)
Q_m	latent heat transferred from water to air (W)
T	temperature (K)
V	volume of the transfer region (m^3)
z	height (m)

Greek symbols

ϕ	relative humidity (-)
ρ	Density (kg m^{-3})
σ	Log-normal standard deviation
ω	humidity ratio (kg kg^{-1})

Subscripts

a	air
CF	counterflow
∞	ambient conditions
i	intermediate
PF	parallel flow
s	saturated
v	vapour
w	water
1	inlet
2	outlet

Abbreviations

CFD	Computational Fluid Dynamics
TC	Tower Characteristic

et al. [14] studied the influence of using different non-uniform layout fillings on the thermal performance of a wet cooling tower. The authors concluded that the cooling efficiency can be improved with different design patterns, roughly between 24% and 30% [13]. Tomás et al. [15] experimentally analysed the performance of new alternative materials for cooling tower fills. The results showed that this type of fills have good potential, since they have a good efficiency compared to industrial fills. They cooled the inlet water by 8 °C (a 20% less than industrial fill). Zhao et al. [16] studied the thermal performance and the resistance characteristics of six types of corrugated film fills. The authors studied the original corrugated fill and five modifications obtained by adding small grooves (number and flow direction). The cooling capacity of the tower was improved by 3.8–12.2% for the optimum fill and empirical formulas for the thermal and resistance characteristics were determined. In Singh and Das [17], the effect of different fill types (wire mesh, honeycomb and wooden splash) on the thermal performance of a forced draft cooling tower was experimentally investigated. Pertinent correlations were developed based on experimental data to simultaneously optimise all performance objectives using the NSGA-II algorithm. The results showed that wire mesh (trickle) fill is the most efficient under the experimental conditions. The same authors also evaluated the performance of cooling towers reported in the literature, in which different fills (Metal splash trays, Rectangular splash bar, Triangular splash bar and Splash) were equipped, in order to validate their model, [18]. Dmitriev et al. [19] experimentally investigated the impact of pack fill on the thermohydraulic performance of an evaporative cooling tower. The fill pack consists of inclined-corrugated contact elements made of perforated metal plates, providing a uniform distribution of interacting phases over the tower's cross-sectional area. It was concluded that the use of certain types of fill packs significantly improves cooling and heat transfer efficiency, especially compared to other types of fill packs. Zhang et al. [20] performed a numerical simulation with non-equidistant fills and non-uniform water distribution in order to synergistically optimise wet cooling towers. Its use decreases the water outlet temperature by around 0.22 °C. Weipeng and Fengzhong [21] compared the cooling characteristics of different fill layout patterns on a single air inlet induced draft cooling tower. It was observed that the average thermal jump of water temperature improved between 0.10 and 0.29 °C.

Concerning the water distribution system, Lemouari et al. [22–24] carried out several experimental studies, to address the thermal performance of a counter-flow wet cooling tower with a VGA (Vertical Grid Apparatus) fill. The authors concluded that the water-to-air mass flow ratio and the temperature of the inlet water were parameters of great importance in thermal performance. Lucas et al. [9] concluded that variation in the water distribution system can increase the thermal performance of the cooling tower by up to 40%. In Ning et al. [25] the thermal performance of a wet cooling tower filled with film packing was investigated under different conditions. The results showed that the tower characteristic is reduced by more than 60% when 15% of the nozzles drop in the cooling tower. Gilani et al. [26] developed a novel, water-efficient configuration for shower cooling tower integrated with the liquid desiccant cooling system. The results showed that reducing the diameter of water drops can reduce the outlet water temperature by up to 5 °C. Dhurandhar and Kanase-Patil [27] conducted an experimental study on the effect of water spray characteristics on cooling tower performance. It was concluded that the full cone angle nozzle (solid spray) has the highest evaporative efficiency (82%).

Lucas et al. [9] studied the thermal performance of a mechanical cooling tower using different drift eliminators and types of water distribution systems. Regarding the drift eliminators, they concluded that the presence of an eliminator does not necessarily worsen the performance of a cooling tower, which is an important aspect. Since, it is normal to think that it does affect, since there is an additional pressure loss incorporated into the air flow. Yu et al. [28] conducted a discussion with the objective of improving the water recovery efficiency using an improved structure of the drift eliminator. With this discussion it was shown that the variation of the geometry of the drift eliminator affects the performance of the cooling tower.

The literature review has highlighted that the fill and the distribution system are the components that have the greatest impact on the thermal performance. Accordingly, the main objective of this paper was to improve the thermal performance of the inverted cooling tower by experimentally optimising the fill length and the distribution system (nozzle position and hydraulic characteristics). The originality of this

(a) Original version, Ruiz et al. [6]. (b) Modified version.

Fig. 1. Experimental facility located in ELDI building, Technical University of Cartagena (Spain).

work is the comparative study between different fills and different distribution systems in this novel device, since no studies of this nature have been reported in the literature up to date. Therefore, this paper fills this literature gap.

This paper is organised into three main sections. Firstly, Section 2 outlines the experimental setup and methodology used for the thermal performance evaluation. Secondly, Section 3 presents and discusses the results obtained from the tests. Finally, Section 4 summarises the key findings of the study.

2. Experimental methodology

2.1. Test facility

A fully instrumented pilot plant consisting of an inverted cooling tower was used to conduct the experiments presented in this paper. The facility is located on the roof of the ELDI building, in the main campus of the Technical University of Cartagena. A primary version of the inverted cooling tower is described in Ruiz et al. [6] and Navarro et al. [29], Fig. 1(a). To experimentally study the influence of the fill length and the distribution system characteristics on the thermal performance of the tower, the facility was slightly modified. The new distribution system consists of 3 manifolds with nine horizontally arranged hollow-cone nozzles. The manifolds (upper, inter-mediate and lower) are placed at 0.7 m, 1.2 m and 1.7 m downwards from the fan, respectively. The hydraulic characteristics of the nozzles are different. In the lower and intermediate levels, the model 3/8 LAP-PP40-40 (Spraying Systems) was used, for a total of 18 units, 9 on each manifold. These nozzles spray the water upwards (Fig. 2(a)). In the upper manifold, the model 3/8 LAP-PP40-20 was used (9 units). These nozzles spray the water downwards due to their proximity to the fan (Fig. 2(b)). Once sprayed, water passes through the trickle-type fill, which is placed between the water nozzles and the tower basin. The fill length is not fixed, since it was varied in the tests to study its influence on thermal performance, as described in Section 2.3. Munters CelDek 7090 pads were used as drift eliminators, placed at the outlet section of the tower. The modified cooling tower is shown in Fig. 1(b).

For the thermal analysis carried out in this work, the measurement of some key variables is required. Fig. 3 shows a schematic representation of the pilot plant shown in Fig. 1(b) including all the sensors used during the experiments.

The variables recorded by the data acquisition system (ECLYPSE, Distech) can be divided into those related to air and water streams and the ambient conditions. Concerning the air stream, the velocity, the temperature and the relative humidity at the inlet and outlet sections of the tower were measured. Eight hot wire anemometers were used to measure the velocity, four placed at the inlet section and one located at the centre of each of the outlet section areas. The temperature and relative humidity of the air were registered using five thermo-hygrometers, one in the inlet section and four in the outlet section. The air mass flow rate was calculated using the average air velocity in the inlet section, the dimensions of the inlet section, and the inlet air specific volume.

Regarding the water stream, the mass flow rate was measured with an electromagnetic flowmeter and the water temperature was recorded at 4 key points: at the inlet (before flowing through the nozzles), in the discharge (tower basin) and inside the tower at two different heights (to measure the temperature in the highest height reached by the water). The conclusions reached by Navarro et al. [29] pointed out that it was necessary to measure the water temperature at these locations in order to discern if the heat and mass transfer occur in counterflow, parallel or counterflow/parallel arrangement. Hence, in order to measure the temperature at this point (where the arrangement of the flows changes) two open water collection channels were installed in the tower. They were placed at different heights so that this measurement would more accurately reflect the temperature at the desired location.

Additionally, a meteorological station (Davis Vantage Pro2), positioned adjacent to the experimental facility, was employed to monitor ambient conditions such as relative humidity, temperature, wind direction and speed.

2.2. Mathematical modelling

The well-known Merkel number is accepted as the performance coefficient of a wet cooling tower, [30–32]. This dimensionless number is defined in Eq. (1), and it measures the degree of difficulty of the mass transfer processes occurring in the exchange area of a cooling tower.

$$\mathrm{Me} = \frac{h_D A}{\dot{m}_w} = \frac{h_D a_v V}{\dot{m}_w} \tag{1}$$

The Merkel number can be calculated using the Merkel and Poppe theories for performance evaluation of cooling towers. The Merkel [33] theory relies on several critical assumptions, such as the Lewis factor being equal to 1, the air exiting the tower being saturated with water vapour and neglecting the reduction of water flow rate by evaporation in the energy balance. For this reason, the Poppe [34]

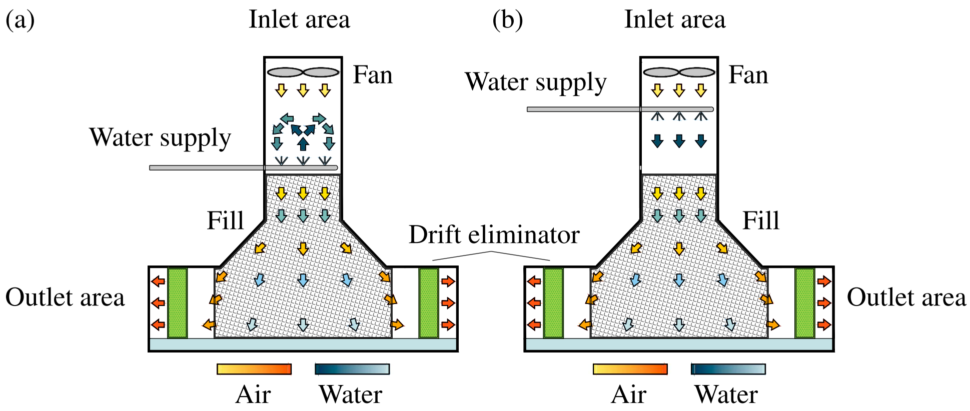

Fig. 2. Schematic of the new prototype of wet cooling tower highlighting the counterflow-parallel flow arrangements and the main parts of the tower. (a) Counterflow-parallel. (b) Parallel.

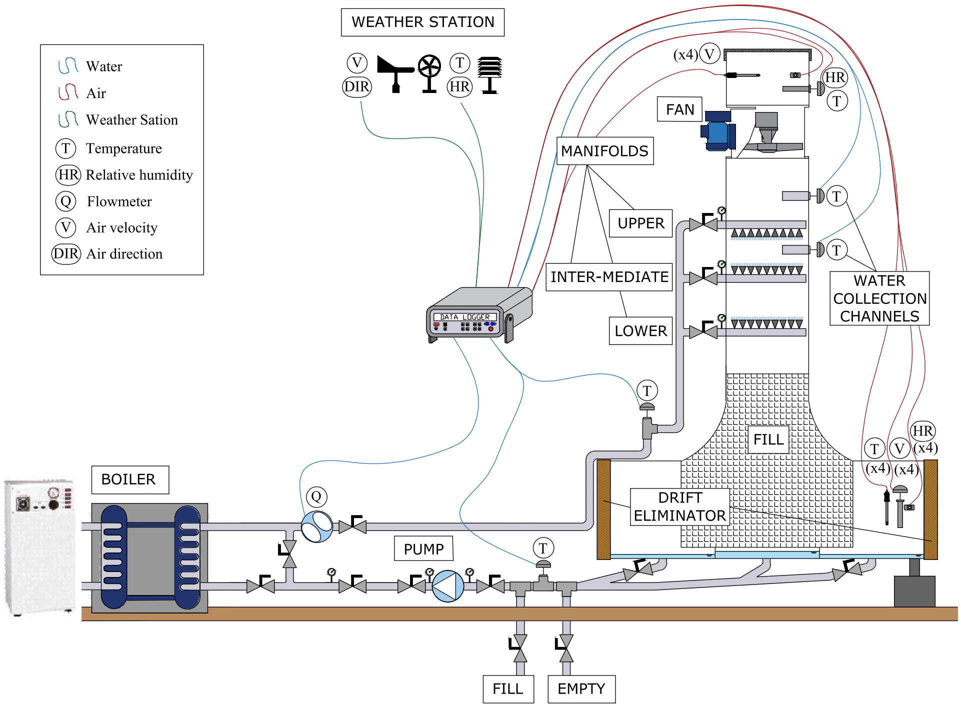

Fig. 3. Schematic of the novel mechanical forced draft counterflow-parallel flow wet cooling tower.

theory is usually preferred. In this theory, the authors derived the governing equations for heat and mass transfer in the transfer region of the cooling tower (control volume shown in Fig. 4, one dimensional problem). The detailed derivation process and simplification of the previously-mentioned governing equations can be found in Navarro et al. [29]

According to the Poppe theory, the major following equations for the heat and mass transfer are obtained:

$$\frac{d\omega}{dT_w} = \frac{c_{p_w}\frac{\dot{m}_w}{\dot{m}_a}\left(\omega_{s_w}-\omega\right)}{\left(h_{s_w}-h\right)+(\mathrm{Le}-1)\left[\left(h_{s_w}-h\right)-\left(\omega_{s_w}-\omega\right)h_v\right]-\left(\omega_{s_w}-\omega\right)h_w} \tag{2}$$

$$\frac{dh}{dT_w} = c_{p_w}\frac{\dot{m}_w}{\dot{m}_a}\left[1+\frac{\left(\omega_{s_w}-\omega\right)c_{p_w}T_w}{\left(h_{s_w}-h\right)+(\mathrm{Le}-1)\left[\left(h_{s_w}-h\right)-\left(\omega_{s_w}-\omega\right)h_v\right]-\left(\omega_{s_w}-\omega\right)h_w}\right] \tag{3}$$

$$\frac{d\,\mathrm{Me}}{dT_w} = \frac{c_{p_w}}{\left(h_{s_w}-h\right)+(\mathrm{Le}-1)\left[\left(h_{s_w}-h\right)-\left(\omega_{s_w}-\omega\right)h_v\right]-\left(\omega_{s_w}-\omega\right)h_w} \tag{4}$$

where the coefficient referred to as Me in Eq. (4), is the Merkel number based on the Poppe theory. These governing equations can be solved using the fourth order Runge–Kutta method. For more information on the calculation process, refer to [29,30] or [35].

The Merkel number, denoted by Me, is calculated differently depending on the arrangement of the water and air flows in the cooling tower. In a typical counterflow cooling tower, water flows downwards while air flows upwards. However, in the inverted cooling tower, water is pumped upwards from the nozzles to the fan until the inertia and drag forces are balanced, and then flows downwards through the fill to be finally collected in the tower basin. Therefore, the flow arrangement is mixed, since part of the cooling takes place in counterflow arrangement and part in parallel arrangement. Fig. 4 shows both flow arrangements, counterflow (Fig. 4(a)) and parallel (Fig. 4(b)).

The influence of the flow arrangement between the water and air streams on the performance of the tower was analysed in Navarro et al. [29]. The authors studied three different flow arrangements: pure counterflow, pure parallel and a combination of counterflow/parallel. They concluded that the approach that combines counterflow and

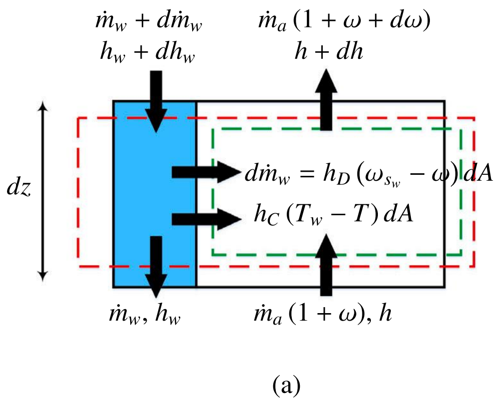

Fig. 4. Control volume in the exchange area of a wet cooling tower. (a) Counterflow and (b) parallel flow arrangements.

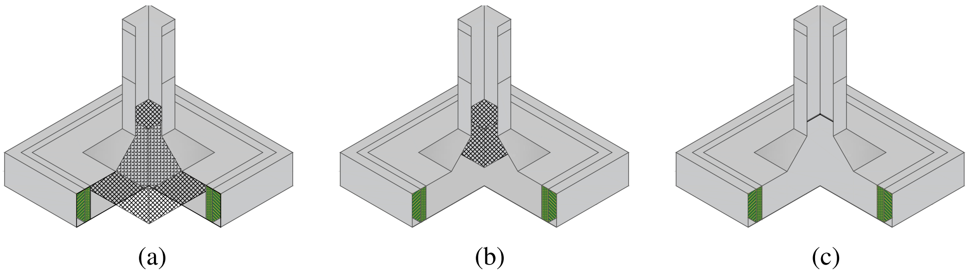

Fig. 5. Arrangement of the fill for the different lengths tested: (a) 1.6 metres, (b) 0.8 metres, (c) no fill.

parallel flow arrangements should be used to evaluate the thermal performance of the inverted cooling tower.

2.3. Experimental procedure

In this investigation, 45 sets of experiments have been carried out with the objective of evaluating the thermal performance of the inverted tower. According to the bibliographic review carried out in Section 1, the two elements with the greatest influence on the thermal efficiency of the tower are the fill and the distribution system (nozzles). The design of the improved inverted tower has 3 levels of spray nozzle manifolds, so the influence of the relative position of the injection, the water–air flow arrangement and the hydraulic characteristics of the nozzle on the thermal performance can be studied.

The thermal performance of the cooling tower was experimentally investigated for three fill lengths (L_f = 1.6 m, L_f = 0.8 m and no fill, Fig. 5) and all the available nozzle manifolds (lower, intermediate and upper manifolds). Concerning the experimental procedure, five sets of experiments for each nozzle manifold and fill length have been performed, for a total of 45 tests.

The five experiments for each combination were obtained by modifying the air flow rate, via the variable frequency drive. Five levels, ranging 10–50 Hz in 10 Hz intervals, were considered. The lowest frequency level of the fan (lowest air flow rate) was selected by ensuring that no water droplets were carried out by the air stream to the inlet section of the cooling tower. Accordingly, if the 10 Hz value was not sufficient, it was increased until there was no drift in the upper section of the tower. To achieve different water-to-air mass flow ratios, a fixed water flow rate of 1.3 kg s^{-1} (under nominal conditions, 50 Hz in the pump variable frequency drive) was maintained. The range of water-to-air mass flow ratios tested in this study was approximately 0.2–1.0. All experiments were conducted at a constant thermal load of 30 kW.

To evaluate the stationary conditions of the tests, it referenced the UNE 13741 "Thermal Performance Acceptance Testing of Mechanical Draught Series Wet Cooling Towers" and CTI "Acceptance Test Code for Water Cooling Towers" standards. The standards require that variations in circulating water flow rate, heat load, and range should not exceed 5%, while wet-bulb temperature and dry-bulb temperature linear least square trends should not exceed 1 °C and 3 °C per hour, respectively. The maximum deviation of the wet-bulb temperature should not exceed its average value during the test period (±1.5 °C). Similarly, for the dry-bulb temperature, a deviation of ± 4.5 °C is acceptable. Additionally, the wind velocity should not exceed 7 m s^{-1} for one minute, and the average value during the test period should not exceed 4.5 m s^{-1}. According to these standards, 1 h of measurement is required for a test to be considered stationary. Tests were conducted during 3–4 h to ensure stationarity and the results were quite consistent.

In summary, for each test a $\dot{m}_w$ (same in all tests), a $\dot{m}_a$ (5 fan frequencies), a fill length (1.6 m, 0.8 m and no fill) and a nozzle manifolds (upper, inter-mediate and lower) were fixed. Fig. 6 schematically represents the configuration of the different tests ($1 \times 5 \times 3 \times 3 = 45$) and the steps taken later during the analysis procedure. Once the variables are fixed, the test is performed and the key parameters are recorded (T_∞, ϕ_∞, T_{w_1}, T_{w_i}, T_{w_2}, $\dot{m}_a$, $\dot{m}_w$). Finally, with these data, the Merkel number is calculated. As mentioned in Section 2.2, in this work the method that uses the Poppe theory and combines counterflow and parallel flow arrangements has been used to evaluate the thermal performance. It should be noted that for the case of spraying from the upper manifold, all the cooling takes place in parallel arrangement. Therefore, the calculation of the Merkel number has been adapted to this configuration. In the intermediate and lower manifolds, the Merkel number has been calculated taking into account the contribution in each of the cooling areas (counterflow and parallel). For this reason, for the water temperature, measurements were taken at three points: inlet (T_{w_1}), intermediate (T_{w_i}) and outlet (T_{w_2}) to independently identify the contributions in countercurrent and parallel arrangements. It is important to mention that during the tests a visual inspection of the water collection channels (located in the upper right area of the tower

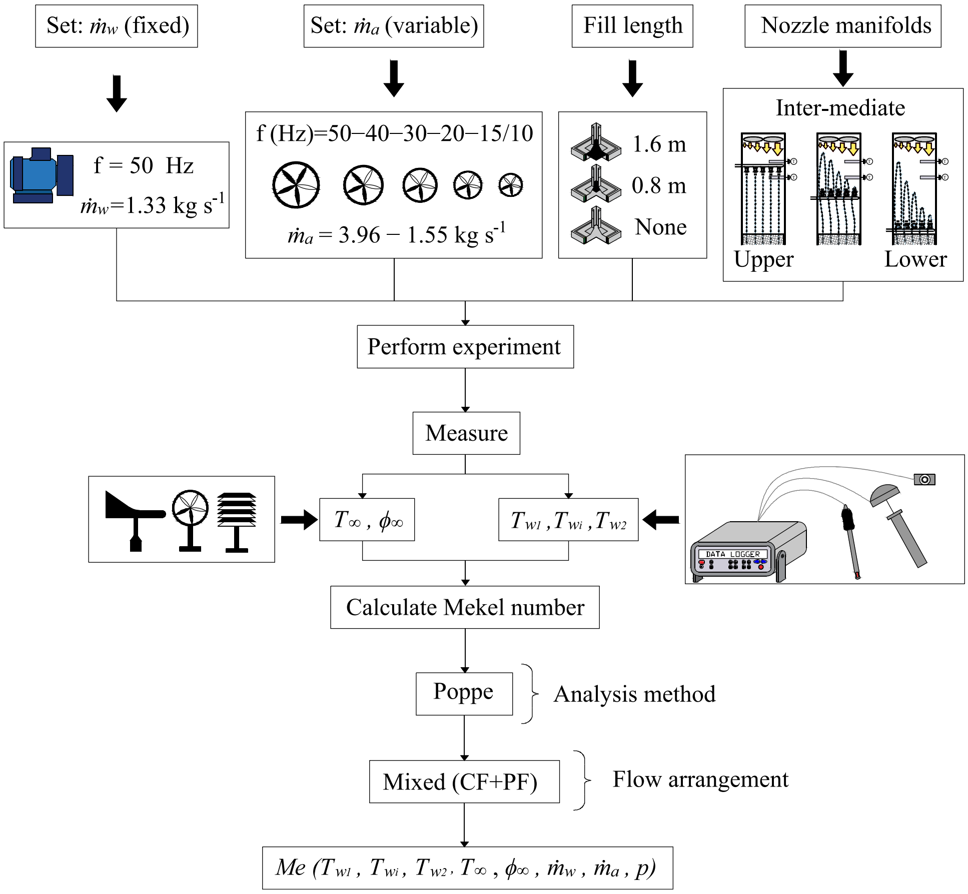

Fig. 6. Experimental procedure flowchart.

shown in Fig. 3) described in Section 2.1 was carried out. For the cases with very high fan frequencies, there are no intermediate temperature measurements, T_{w_i}, since the water did not reach the channels.

3. Results and discussion

3.1. Experimental results

The experimental results obtained for the 45 tests described in Section 2.3 are presented in this section.

Tables 1, 2 and 3 contain the average values for the variables used to calculate the Merkel number (environmental conditions and tower operating conditions) for all manifolds and all fill lengths studied. These tables also include the experimental results obtained for the Merkel number (counterflow, parallel and mixed) and the water-to-air mass flow ratio. The results have been calculated as described in Section 2.3.

The environmental conditions present some variations due to the fact that the tests were carried out during different months. These conditions are typical of a Mediterranean climate, and range between 17.67 °C and 30.59 °C for ambient temperature, and between 16.88% and 93.42% for relative humidity. As already mentioned, the water mass flow rate was maintained constant during the tests (around 1.33 kg s^{-1}), while the air mass flow rate was modified between 1.43 and 6.29 kg s^{-1} for the different tests carried out.

The results of the experimental investigation on the variation of Merkel number with the water-to-air mass flow ratio for all manifolds, fill lengths, and water-to-air mass flow ratios studied are presented in Fig. 7. The obtained results reveal the expected trend of decreasing Merkel number potentially with an increase in the water-to-air mass flow ratio, following a linear trend on a log–log scale. This trend is observed for all fill lengths and manifolds studied. Furthermore, it is evident that the Merkel number differs for different cases analysed even when the water-to-air mass flow ratio is kept constant. This observation supports the initial hypothesis of the influence of fill and water distribution system on the heat and mass transfer processes occurring in the cooling tower. As it can be seen, the sequence for the fill lengths in terms of better thermal efficiency is 1.6 m, 0.8 m and no fill whereas concerning the manifold position is upper, intermediate and lower.

In [29], the experimental uncertainty was assessed following the ISO Guide [36] with a coverage factor of $k = 2$ (95% level of confidence) for the expanded uncertainty and type B evaluation for standard uncertainty. Averaged values of 3.53%, and 11.73% were obtained for $\dot{m}_w/\dot{m}_a$ and Me, respectively.

3.2. Contribution of each flow arrangement

As explained before, in the lower and intermediate manifolds part of the cooling takes place in the parallel flow arrangement. Therefore, the first discussion that can be carried out is to analyse the contribution of each flow arrangement to the total Merkel number. Fig. 8 shows the fraction of the total cooling taking place in counterflow arrangement ($\mathrm{Me_{CF}} / \mathrm{Me_{CF+PF}}$), being the total Merkel number $\mathrm{Me_{CF+PF}} = \mathrm{Me_{CF}} + \mathrm{Me_{PF}}$.

As it can be seen, the results are quite different between the intermediate and lower manifolds. Concerning the different fill lengths, no significant differences are observed.

In the case of the intermediate manifold, the cooling process is a mix of counterflow and parallel arrangements for intermediate fan

Table 1
Averaged values in the thermal experimental test runs with the upper manifold.

Fill	f (Hz)	T_∞ (°C)	ϕ_∞ (%)	T_{w_1} (°C)	T_{w_i} (°C)	T_{w_2} (°C)	$\dot{m}_a$ (kg s^{-1})	$\dot{m}_w$ (kg s^{-1})	$\dot{m}_w/\dot{m}_a$	Me_{CF}	Me_{PF}	Me_{CF+PF}
	50	25.48	76.98	31.19	–	26.17	4.6130	1.3959	0.3026	0.0000	1.0725	1.0725
	40	25.95	82.02	32.90	–	27.92	4.0690	1.3964	0.3432	0.0000	0.8891	0.8891
1.6 m	30	25.75	82.30	34.63	–	29.62	3.1006	1.4018	0.4521	0.0000	0.6577	0.6577
	20	25.28	80.33	35.47	–	30.48	2.6026	1.3944	0.5358	0.0000	0.5422	0.5422
	10	25.78	76.60	40.84	–	35.76	1.4467	1.4037	0.9703	0.0000	0.3163	0.3163
	50	19.51	59.85	23.78	–	19.76	5.1274	1.3509	0.2635	0.0000	0.9204	0.9204
	40	19.68	57.87	24.76	–	20.75	4.2698	1.3567	0.3178	0.0000	0.7774	0.7774
0.8 m	30	20.70	45.07	26.18	–	22.23	3.5777	1.3825	0.3864	0.0000	0.5676	0.5676
	20	20.64	77.53	30.95	–	27.02	2.8567	1.3878	0.4858	0.0000	0.4520	0.4520
	10	21.29	78.35	35.62	–	31.67	1.8840	1.3832	0.7342	0.0000	0.2931	0.2931
	50	25.61	69.67	30.12	–	24.80	6.2855	1.3407	0.2133	0.0000	1.2122	1.2122
	40	25.77	71.12	31.44	–	26.18	5.2138	1.3845	0.2655	0.0000	0.9626	0.9626
None	30	28.63	31.32	30.06	–	24.78	3.5306	1.3657	0.3868	0.0000	0.7201	0.7201
	20	28.34	25.77	32.61	–	27.24	2.8050	1.3703	0.4885	0.0000	0.4991	0.4991
	10	28.25	16.88	36.86	–	31.57	1.7787	1.3675	0.7688	0.0000	0.3162	0.3162

Table 2
Averaged values in the thermal experimental test runs with the inter-mediate manifold.

Fill	f (Hz)	T_∞ (°C)	ϕ_∞ (%)	T_{w_1} (°C)	T_{w_i} (°C)	T_{w_2} (°C)	$\dot{m}_a$ (kg s^{-1})	$\dot{m}_w$ (kg s^{-1})	$\dot{m}_w/\dot{m}_a$	Me_{CF}	Me_{PF}	Me_{CF+PF}
	50	28.47	71.78	33.39	–	28.13	3.9575	1.3151	0.3323	0.0000	1.0320	1.0320
	40	26.25	77.82	34.36	–	29.23	2.9699	1.3137	0.4423	0.0000	0.7035	0.7035
1.6 m	30	27.36	62.97	36.02	31.33	30.67	2.5029	1.3088	0.5229	0.4070	0.0726	0.4796
	25	27.33	74.83	40.35	36.84	34.95	2.0922	1.3154	0.6287	0.1980	0.1375	0.3355
	15	30.59	61.97	49.78	49.78	45.37	1.5488	1.3241	0.8549	0.0000	0.1255	0.1255
	50	22.60	82.68	29.28	–	25.14	4.2610	1.3139	0.3083	0.0000	0.8070	0.8070
	40	24.32	53.43	28.42	–	24.33	3.5563	1.3099	0.3683	0.0000	0.6581	0.6581
0.8 m	30	24.85	61.97	32.46	28.75	28.28	2.8102	1.3136	0.4674	0.3787	0.0582	0.4370
	20	24.35	65.67	41.09	39.83	37.06	2.1797	1.3211	0.6061	0.0499	0.1325	0.1824
	14	21.43	32.80	40.60	40.60	36.54	1.4689	1.3242	0.9015	0.0000	0.1634	0.1634
	50	25.41	79.10	29.91	–	25.78	5.2691	1.2688	0.2408	0.0000	1.0108	1.0108
	40	26.16	76.52	31.98	–	27.67	4.1963	1.2686	0.3023	0.0000	0.7319	0.7319
None	30	24.95	85.43	34.34	31.02	30.22	3.1494	1.3005	0.4129	0.3401	0.1044	0.4445
	20	25.21	83.98	41.80	38.89	37.58	2.0326	1.2914	0.6353	0.1347	0.0714	0.2061
	15	25.32	81.93	43.54	43.54	39.41	1.6688	1.2894	0.7726	0.0000	0.1801	0.1801

Table 3
Averaged values in the thermal experimental test runs with the lower manifold.

Fill	f (Hz)	T_∞ (°C)	ϕ_∞ (%)	T_{w_1} (°C)	T_{w_i} (°C)	T_{w_2} (°C)	$\dot{m}_a$ (kg s^{-1})	$\dot{m}_w$ (kg s^{-1})	$\dot{m}_w/\dot{m}_a$	Me_{CF}	Me_{PF}	Me_{CF+PF}
	50	27.58	82.10	34.58	–	29.20	4.0566	1.3142	0.3240	0.0000	0.9249	0.9249
	40	28.12	80.73	36.40	–	31.01	3.2528	1.3113	0.4031	0.0000	0.6930	0.6930
1.6 m	30	26.16	77.52	37.65	–	32.27	2.6555	1.3026	0.4905	0.0000	0.4623	0.4623
	20	25.78	79.13	44.88	–	39.74	2.3556	1.3154	0.5584	0.0000	0.2082	0.2082
	15	29.72	58.55	47.87	47.46	43.13	1.4266	1.3135	0.9207	0.0106	0.1420	0.1525
	50	21.68	68.32	27.53	–	23.44	4.2653	1.2929	0.3031	0.0000	0.7356	0.7356
	40	18.87	65.38	27.01	–	22.85	3.7170	1.3016	0.3502	0.0000	0.6061	0.6061
0.8 m	30	19.04	69.73	30.03	–	25.99	2.9760	1.3070	0.4392	0.0000	0.4309	0.4309
	20	17.67	31.70	41.03	40.90	36.92	2.4320	1.3067	0.5373	0.0039	0.1427	0.1466
	14	17.85	48.15	41.84	41.26	37.82	1.6336	1.3016	0.7968	0.0178	0.1254	0.1432
	50	24.60	81.80	30.69	–	26.53	4.6396	1.2799	0.2759	0.0000	0.7942	0.7942
	40	25.57	76.68	32.16	–	27.99	3.7387	1.2852	0.3438	0.0000	0.6310	0.6310
None	30	25.05	79.90	35.10	–	30.85	2.7878	1.2832	0.4603	0.0000	0.4217	0.4217
	20	24.88	81.30	41.78	–	37.59	2.0325	1.2895	0.6344	0.0000	0.2073	0.2073
	15	21.94	93.42	48.17	–	44.74	1.8542	1.2879	0.6946	0.0000	0.0948	0.0948

frequencies. However, for high fan frequencies (f > 40 Hz) and low frequencies ($f \approx 15$ Hz), the cooling is mainly carried out in parallel arrangement. On the other hand, for the lower manifold, cooling mostly occurs in parallel arrangement for high fan frequencies (f > 30 Hz) while it is only mixed for low frequencies (f < 30 Hz). This is justified for two reasons: the available distance for heat and mass exchange and the position of the collection channels.

For high fan frequencies there is only cooling in parallel arrangement. This is justified because the highest height reached by the water (where the arrangement of the flows changes) is very close to the position of the nozzles and therefore the water does not reach the channels. For this reason, it is assumed that the cooling occurs in parallel (there is a small part of counterflow cooling that cannot be measured). This is illustrated graphically on the rightmost side of the volumes shown in Fig. 9 (red-shaded areas). When the frequency of the fan decreases, water begins to reach the channels and it is possible to measure the amount of counterflow and parallel cooling. As already mentioned, this phenomenon occurs for higher frequencies for the intermediate manifold than for the lower manifolds, which is justified by the distance between the nozzles and the channels in both cases. Finally, for the lower fan frequency levels tested, the water reaches the channels without changing its temperature (intermediate manifold) or with a value very close to the inlet temperature (lower manifold), probably due to the short time required to reach the maximum height. Therefore, for these cases the counterflow cooling is zero (intermediate manifold) or almost zero (lower manifold) and all or almost all cooling

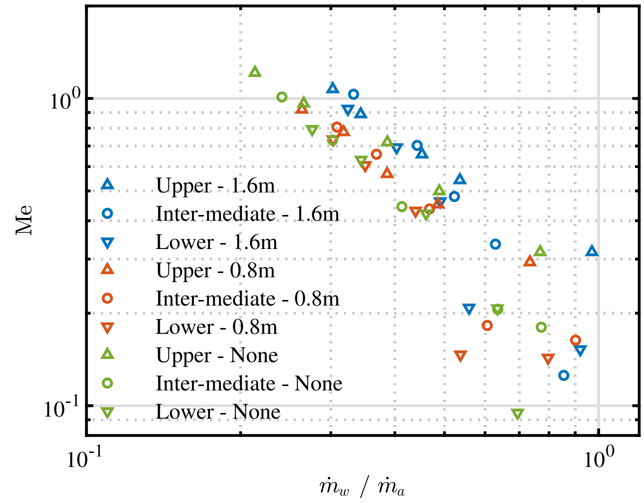

Fig. 7. Experimental results for the Me number as a function of $\dot{m}_w/\dot{m}_a$.

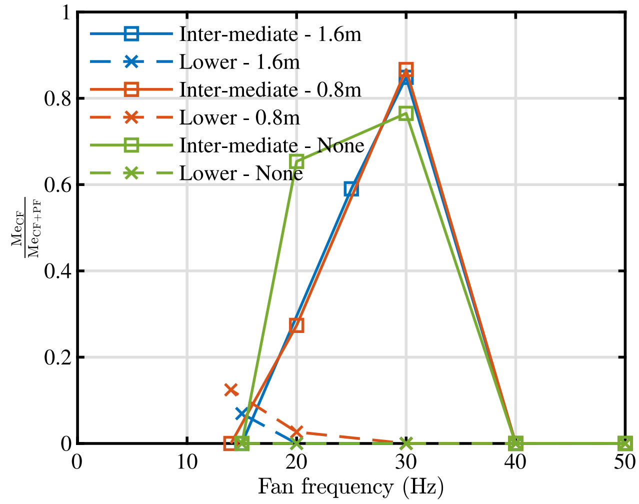

Fig. 8. Contribution of the counterflow arrangement as a fraction of the total cooling as a function of fan frequency.

occurs in parallel. This behaviour is explained on the leftmost side of the volumes shown in Fig. 9 (yellow-shaded area).

3.3. Influence of the fill length on the thermal performance

The left-hand side of Fig. 10 shows the comparison between the three fill lengths for each of the three manifolds. The sequence in terms of thermal performance is $Me_{L_f=1.6\ m} > Me_{L_f=0.8\ m} \sim Me_{L_f=0\ m}$ regardless of the manifold analysed. The change in Me with L_f can be explained by two distinct physical phenomena, one linked to the increase of a_V and the other associated with the modification of the h_D coefficient, as expressed in Eq. (1). The a_V parameter denotes the heat and mass exchange surface area per unit volume of the tower, while h_D refers to the mass transfer coefficient.

Increasing L_f increases the contact time and surface between the two fluids, improving the thermal performance via the a_V term. That is why the performance for $L_f = 1.6$ m is higher than the others fill lengths. The relative importance of both physical phenomena described above explains the small variation of Me for $L_f = 0.8$ m and no fill. On the one hand, the extra exchange area makes the term a_V higher for the case with 0.8 fill length. It should be noted, however, that the amount of fill volume introduced compared to 1.6 m is roughly 9 times less (3.70 dm^3 vs 32.58 dm^3). On the other hand, the h_D coefficient is greater in the case with no fill because of the fact that the air velocity is higher. As a consequence, the contribution of one variable is offset by the other. It should be also noted that the experimental uncertainty could be affecting the discussion since the difference between the Merkel numbers for these cases is very small.

Table 4
Averaged and maximum difference in terms of Merkel number correlated between fill length for every available manifolds.

Manifolds	Fill compared	Averaged difference (%)	Max difference (%)
Upper	1.6 m – 0.8 m	26.80	29.71
	1.6 m – None	17.13	17.72
	0.8 m – None	−11.32	−14.63
Inter-mediate	1.6 m – 0.8 m	19.26	−41.23
	1.6 m – None	28.43	48.78
	0.8 m – None	8.64	13.54
Lower	1.6 m – 0.8 m	30.45	32.00
	1.6 m – None	31.65	37.55
	0.8 m – None	1.80	−8.86

To qualitatively compare the influence of the fill length on the thermal performance, Table 4 depicts the difference, averaged and maximum, in terms of Merkel number, between fill lengths for all the manifolds. The averaged difference was obtained by evaluating the Merkel number in 5 water-to-air mass flow ratios ranging between the maximum and minimum values obtained in the experiments and averaging those results. The largest discrepancy was determined for the water-to-air mass flow ratio that resulted in the highest variation between Merkel numbers. It can be observed that, in some cases, the calculated deviations are negative. This means that the second of the fills in column 2 outperforms the first. Results show an average difference between 1.6 and 0.8 m of fill length of around of 25.5%. However, in the case of 0.8 m and without fill, the difference is very low around 0.3%. In the upper manifold it is above even.

3.4. Influence of the distribution system on the thermal performance

The right-hand side of Fig. 10 shows the comparison between the three manifolds for all the fill lengths tested. The first conclusion that can be reached is that, generally speaking, the upper manifold offers the best performance followed by the intermediate and the lower manifolds. However, this trend is reversed for some water-to-air mass flow ratios and Me tends to converge at the same point for the three manifolds, the sequence being Inter-mediate ≈ Lower ≈ Upper.

This is justified according to the following hypothesis. For low $\dot{m}_w/\dot{m}_a$ levels, the cooling occurs in parallel for the three manifolds and, therefore, the difference between them is negligible. The small differences between the intermediate and lower manifolds with the upper could be explained because in cases where water is sprayed upwards, the drops fall in parallel with less inertia than when sprayed directly downwards (upper manifold) and therefore the contact time is larger. However, this is offset by better performance of the upper manifold nozzles, which have better characteristics. Hence the results are very similar. For high $\dot{m}_w/\dot{m}_a$ levels (minimum fan frequency), the benefit of using the upper manifold is justified by its better spraying characteristics (higher coefficient a_V), which should result in a better performance despite the fact that for the parallel arrangement there are less uniform temperature and concentration differences between the fluids over the entire length of the fluid path. Also, although there is a large section in countercurrent (Fig. 9), the water reaches the highest height of the tower without cooling ($T_{w_1} = T_{w_i}$). Therefore, all the cooling occurs in parallel, with the exception that for the intermediate and lower manifolds, the air that reaches the fill is more saturated due to the interaction with water than the case of the upper manifold. For the upper manifold, the exchange air is in ambient conditions, while in

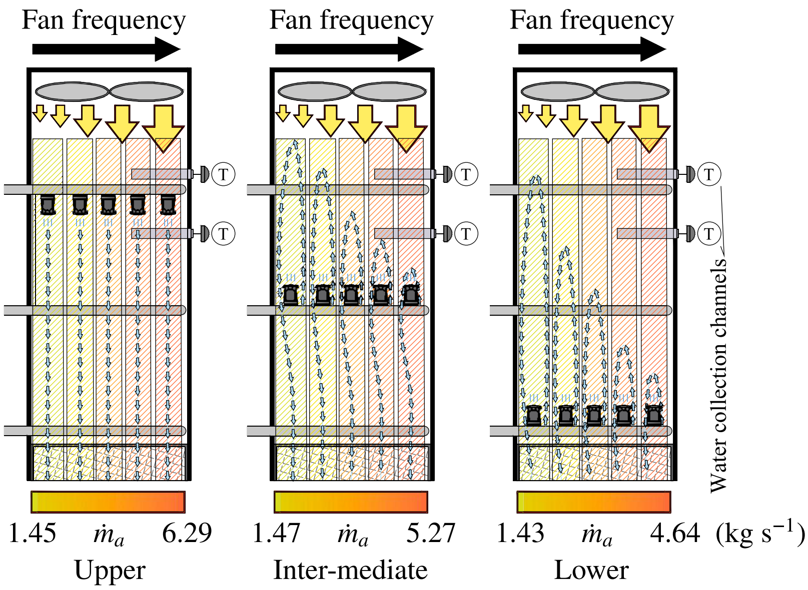

Fig. 9. Channel location and flow arrangement.

Table 5
Averaged and maximum difference in terms of Merkel number correlated between available manifolds for every fill length.

Fill	Manifolds compared	Averaged difference (%)	Max difference (%)
1.6 m	Upper–Intermediate	26.06	−57.73
	Upper–Lower	39.12	59.90
	Intermediate–Lower	13.17	−29.28
0.8 m	Upper–Intermediate	17.69	−33.50
	Upper–Lower	34.66	53.14
	Intermediate–Lower	23.05	30.97
None	Upper–Intermediate	31.17	47.37
	Upper–Lower	37.56	−61.78
	Intermediate–Lower	12.25	−30.94

Table 6
Constants c and n for the different configuration used.

Fill	Manifolds	c	n
1.6 m	Upper	0.2971	1.0338
	Inter-mediate	0.1042	2.2227
	Lower	0.1114	1.8480
0.8 m	Upper	0.2024	1.1351
	Inter-mediate	0.1147	1.6534
	Lower	0.0748	1.9038
None	Upper	0.2433	1.0513
	Inter-mediate	0.1124	1.5467
	Lower	0.0634	2.1024

the rest of the manifolds it is air that has already been moistened by the heat exchange in the counterflow section. That is why the upper manifold performance is best for these operating conditions. Finally, the better performance of the intermediate manifold compared to the lower can be explained by a higher coefficient a_V due to the wetted surface of the manifold (pipes) located below, as well as the length available for exchange, which also increases the coefficient a_V.

Table 5 depicts the difference, averaged and maximum, in terms of Merkel number, between available manifolds for every fill length. Results show an average difference between Lower and Upper manifolds of around of 37.12% and around of 24.97% for Inter-mediate and Upper manifolds. In the case of Lower and Inter-mediate manifolds, the difference is around of 16.16%.

3.5. Correlation and validation (water and air outlet temperature prediction)

As described in [9,30,37], to correlate the values of the Merkel number of a tower, it is common to use the ratio of water-to-air mass flow ratio as an independent variable, described by an equation of the form $\mathrm{Me} = c\left(\dot{m}_w/\dot{m}_a\right)^{-n}$. Constants c and n in the previous equation are presented in Table 6. These coefficients are obtained by performing a power-law fit of the data of $\dot{m}_w/\dot{m}_a$ and Me shown in Fig. 10 (linear trend on a logarithmic scale).

The solid lines in Fig. 10 correspond to the transfer characteristics of the different configurations tested on the cooling tower. In order to evaluate the goodness of the correlation, the difference between calculated and measured outlet water temperatures was compared. This is possible because with the obtained fitting parameters (c and n), Me can be predicted for a known value of $\dot{m}_w/\dot{m}_a$. As explained in Fig. 6, if Me and the rest of the variables (T_∞, ϕ_∞, T_{w_1}, $\dot{m}_a$, $\dot{m}_w$ and p) are known (experimental test data), it is possible to calculate the missing variable (T_{w_2}) and verify that it matches the experimentally measured value. As shown in Table 7, an averaged deviation of 0.37 °C (1.07%) was observed between the calculated and predicted temperatures. The goodness of these data has also been analysed through statistical methods, to corroborate their acceptance. The Root Mean Square Error (RMSE) and R-squared (R^2) have been calculated, being the averaged and most unfavourable values obtained: $R^2 = 0.9997$ and RMSE = 0.4768, and $R^2 = 0.9907$, RMSE = 1.0197, respectively. In light of this, it can be concluded that Ashrae's correlation alongside with the Poppe method predict the thermal performance of the cooling tower well because the predicted results are remarkably confident. Fig. 11 shows as an example, the calculated and experimental outlet water temperatures for all the tests.

As can be seen, the differences are very low and the models fit very well (Table 7) for all the configurations tested. The goodness of the fits is better for the upper manifold than for the other manifolds. The explanation given is that in the upper manifold there is no change between counterflow and parallel arrangement, and the Merkel number calculation is straightforward. In addition, Fig. 11 shows that the cases with high temperatures provide the worst results. Those cases coincide with the highest water-to-air mass flow ratios, when is more difficult to discern between parallel and counterflow cooling. Hence the worse

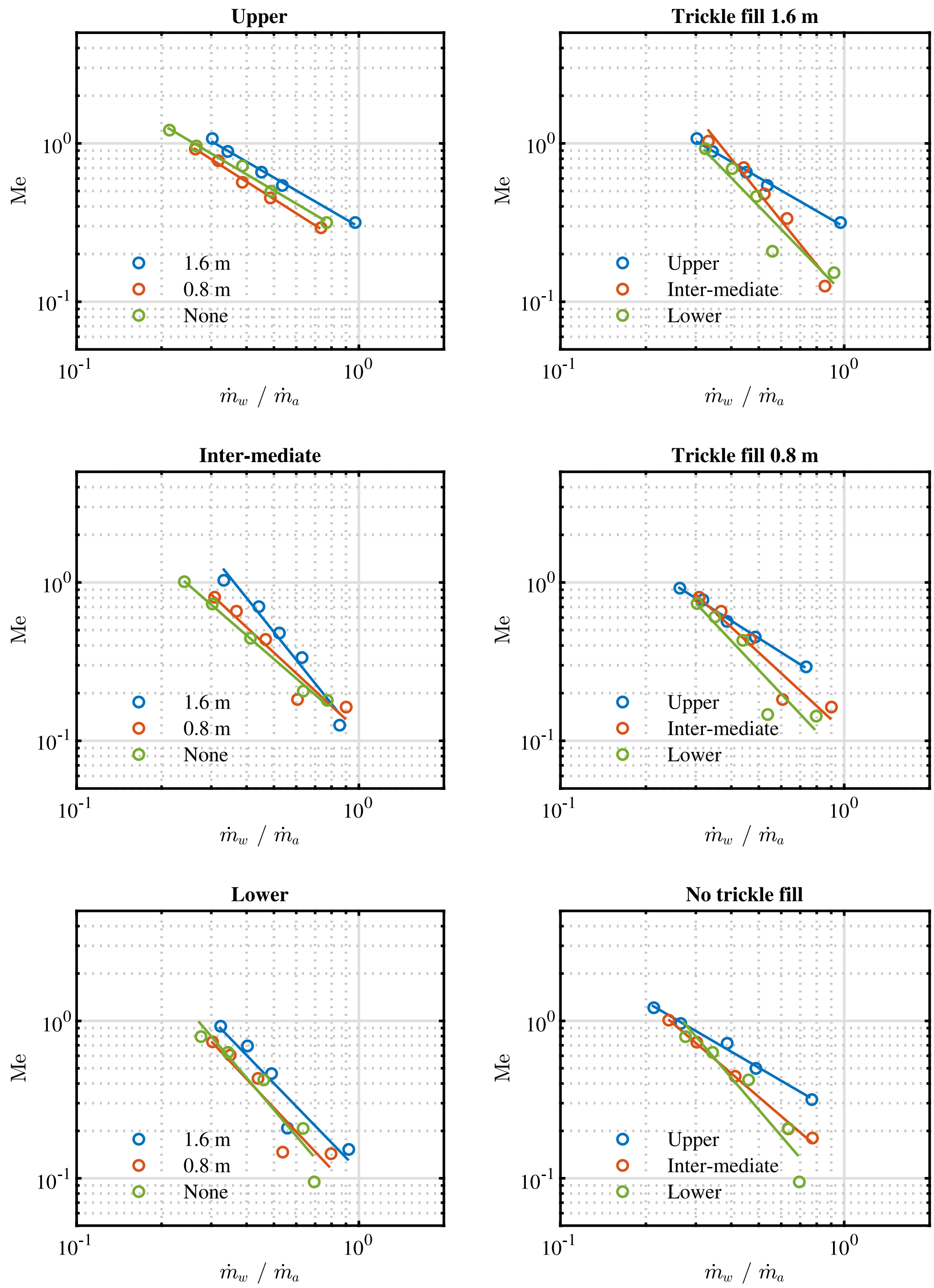

Fig. 10. Cooling tower Merkel number as a function of water-to-air mass flow ratio for the three fill lengths and three available nozzle manifolds. Left-hand side:influence of fill length. Right-hand side: influence of nozzle manifold.

fit and the larger the difference between experimental and predicted results.

The Poppe method is capable of providing the air profiles (enthalpy and humidity ratio) during the transfer process of the cooling tower, so it is possible to know the evolution of the air properties and its conditions at the outlet (temperature and humidity). These results have been represented in a psychrometric chart (Fig. 12) for four different experimental tests (different manifolds, fill lengths and flow arrangements). As the effectiveness of evaporative cooling relies on the difference between the enthalpy of air and the enthalpy of saturated air calculated at the water temperature, Fig. 12 shows the evolution of water with a solid line overlapping the saturation curve.

As it can be seen, the air increases its moisture contents and is heated up while evolving to the outlet water temperature in all cases. However, some differences are highlighted. For example, for the cases of higher frequency (f = 50 Hz), it is observed that the temperature evolution is shorter than for the cases of lower frequency. This is because there is less contact time between water and air due to the large air velocity. It can also be seen that for some cases (yellow-shaded area in Fig. 12), the air temperature near the outlet section of the cooling tower is higher than the water temperature at that point ($T_a > T_w$). This means that the transfer of sensible heat occurs from the air to the water, while the transfer of latent heat occurs from the water to the air. However, the net transfer of enthalpy still occurs in the direction of the air. This process results in cooling of both the air and water in this area.

On the other hand, as already explained for intermediate frequencies (f = 25 Hz), the cooling occurs in two different flow arrangements,

Table 7
Averaged and maximum difference in number of correlated Me between different configurations used.

Fill	Manifolds	Max difference (°C)	Averaged difference (°C)
1.6 m	Upper	0.13	0.09
	Inter-mediate	0.60	0.41
	Lower	1.94	0.68
0.8 m	Upper	0.13	0.07
	Inter-mediate	1.36	0.48
	Lower	2.10	0.72
None	Upper	0.27	0.11
	Inter-mediate	0.34	0.13
	Lower	1.22	0.64

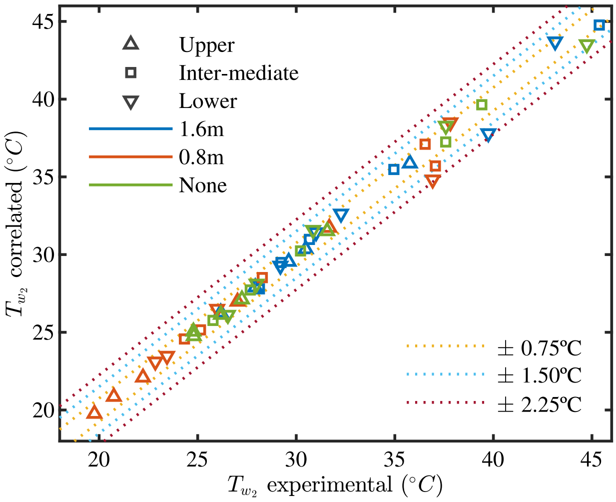

Fig. 11. Comparison between experimental and predicted cooling tower outlet water temperature for all cases.

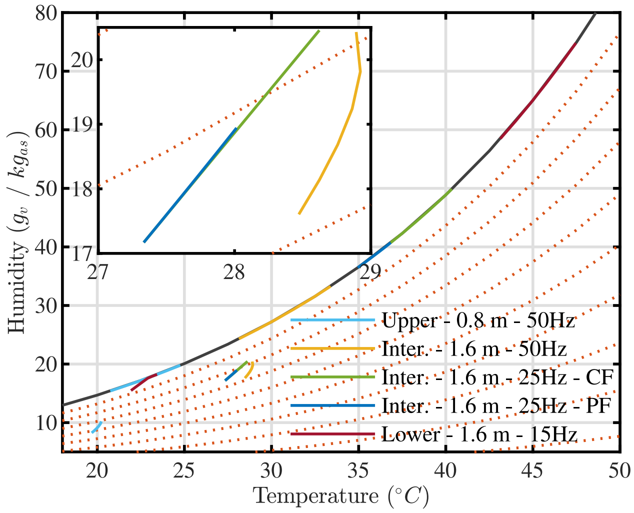

Fig. 12. Evolution of the properties of water and air in a psychrometric chart.

therefore, the evolution of the air in both arrangements is shown in different colours (green and dark blue). In this case, the air conditions coincide at the entrance, however, in each case heat is exchanged with different water temperatures. Finally, in the red series, another particular situation is observed. In this case, there is a high humidity at the inlet, so that, when the exchange process begins, there is a point where the air saturates and therefore, the evolution of the air conditions follows the line marked by the saturated air conditions.

As for the air temperature at the cooling tower exit area, the Poppe model is also quite reliable for its calculation. The results of the 45 tests shown here establish an average difference of 1.35 °C (4.93%). These differences are very low for high fan frequency values. However, as it decreases, the difference increases. The explanation given to this fact is related to the air temperature distribution at the outlet section being less uniform for decreasing fan frequency values and measuring in one single point.

In view of the results obtained, it can be said that it is important to define well the amount of fill to be used. In the same way, that the spraying position for a particular tower like the one studied. The results showed that the upper manifold presents the best performance, but also revealed that for some operating ranges of the tower (design conditions), it is possible that the intermediate and lower manifolds present better performance. In this sense, a modification of the pump would allow to know more data in this regard. Finally, it has also been observed that using fixed channels to determine the water temperature when it changes arrangement is a limitation. Therefore, if this is modified, the performance of the new prototype could be better characterised, beyond the fact that the proposed models predict practically identical water and air outlet temperatures.

3.6. Comparison with the original version and experimental data available in the literature

In order to contextualise the tower's performance, the best results obtained in this study (L_f = 1.6 m) were compared with the original version of the inverted cooling tower [6], as well as other towers referenced in the bibliography [9,38–41].

The thermal performance of investigated towers is compared in Fig. 13, where Fig. 13(a) displays the Merkel number comparison. Curves for the different towers under consideration have been plotted against constant approach curves.

The approach of a cooling tower is a crucial parameter to assess its performance. It represents the difference between the outlet cold water temperature and the ambient air wet bulb temperature. In this regard, the constant approach curves were computed for the design operating conditions of the inverted cooling tower, where a wet-bulb temperature of 27 °C and a range of 5 °C were considered. These curves provide valuable information about the tower's performance under different conditions. The constant approach curves' shape is dictated by the $\dot{m}_w/\dot{m}_a$ ratio. In the hypothetical scenario where the air rate is infinite, $\dot{m}_w/\dot{m}_a = 0$, which corresponds to the maximum driving force and the minimum required Merkel number. As the air rate decreases, the driving force decreases, and the required Merkel number increases. The intersection points between the constant approach curves and the tower performance curves ($\text{Me} = c\left(\dot{m}_w/\dot{m}_a\right)^{-n}$) indicate the $\dot{m}_w/\dot{m}_a$ values at which the towers will operate for the given conditions.

Regarding the comparison of Merkel number, it was observed that for high water-to-air mass flow ratios ($0.3 < \dot{m}_w/\dot{m}_a$), the inverted cooling tower has a lower performance than the commercial cooling towers. However, for low water-to-air mass flow ratios ($\dot{m}_w/\dot{m}_a < 0.3$), the new design shows better performance compared to the commercial towers reported in the literature. Something similar happens if the results are compared with the original version of the inverted tower, [6]. On the one hand, the hydraulic resistance of the original nozzles was different from the new ones (higher coefficient a_v), and on the other hand, the new manifolds (pipes) located below increase the wetted surface (higher coefficient a_V).

While the Merkel number is an effective metric when comparing the performance of wet cooling towers, its use may not always provide clear insight into the energetic implications of different designs. The key parameter for predicting the performance of a system that incorporates a cooling tower for heat removal (such as a power cycle or refrigeration cycle) is the outlet water temperature. Therefore, the outlet water temperatures for the previously cited cooling towers are also predicted for three different levels of $\dot{m}_w/\dot{m}_a$ (0.2, 0.7, and 1.2). Fig. 13(b) illustrates the projected outlet water temperatures for the

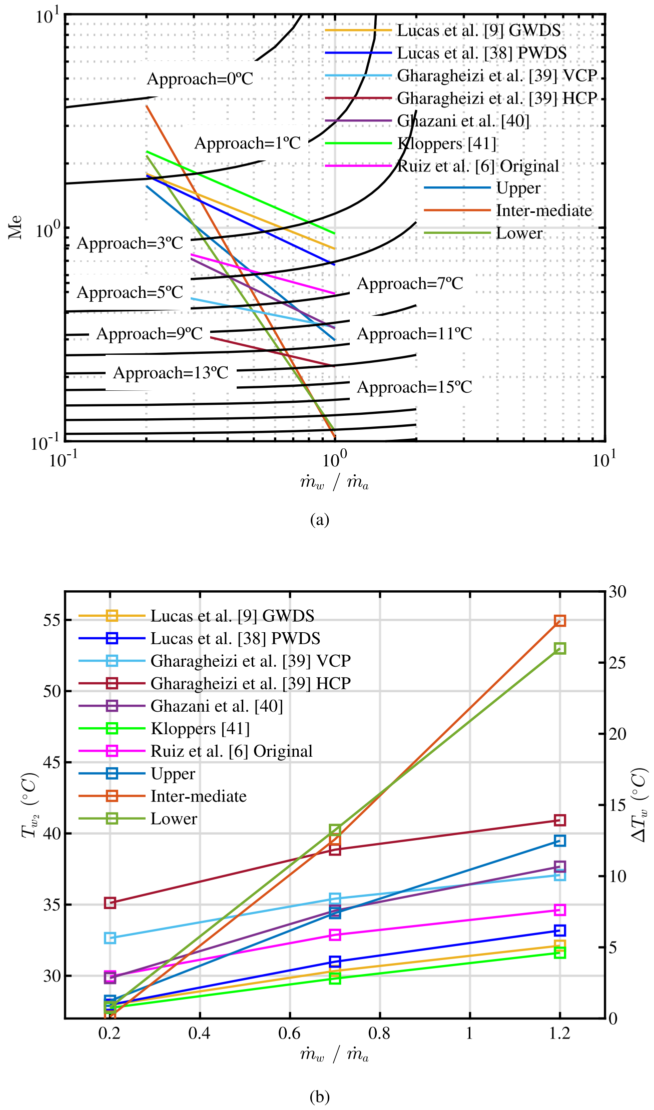

Fig. 13. Comparison between the experimental data obtained in this research and the data reported in the literature [6,9,38–41]. (a) Me number and (b) T_{w_2} for the specified conditions.

bibliographic results considered in this section. As an example, with the inverted cooling tower (upper manifold) and $\dot{m}_w/\dot{m}_a = 0.5$, an approach of approximately 5 °C is achieved. This corresponds to a water outlet temperature of approximately 32 °C.

Finally, some remarks are made concerning the influence of the distribution system and fill length on the drift emissions level. Preliminary drift tests have been conducted, considering the various configurations outlined in this paper. The results of these preliminary tests indicate that the drift rates vary from 0.00015% to 0.00022%. As such, no significant differences have been observed between the initial tower prototype (0.00015%, Ruiz et al. [6]) and the modifications to the fill length and distribution system analysed in this paper. A detailed analysis of the drift results will form part of future investigations yet to be published.

4. Conclusions

This study has enabled investigating the effect of the fill length and the distribution system (nozzle position and hydraulic characteristics) on the thermal performance of a modified novel type of inverted cooling tower. The findings of the study can be concisely presented as follows:

The spray characteristics and the manifold position has been found to be the most important parameters affecting the tower performance. The upper manifold is, in the light of the obtained results, the best configuration for all mass flow ratios in which the tower works (25% better than the intermediate manifold and 37% better than the lower manifold). This is because at first it was considered that the upper manifold would have worse results (parallel flow), so better nozzles were installed. However, in view of the results, the nozzles chosen should be those installed on the upper level, although possibly installed on the other levels will obtain better results. Since the combination of a higher nozzle hydraulic resistance and a larger surface area of exchange (lower manifold) could result, in the light of the obtained results, in the best configuration.

The fill has influence on all manifolds operation in a similar way, since all the cooling takes place in the parallel flow arrangement for almost all of them. The performance for the 1.6 m length of fill is 25.5% better than for the other two lengths tested. The main conclusion in this regard is that installing a large amount of fill clearly improves the performance of the tower, but installing a small amount does not always compare to installing nothing.

Ashrae's correlation alongside the Poppe method successfully predict the thermal performance of the cooling tower well. The average difference found between experimental and predicted results is 0.37 °C. In addition, Poppe's method is able to predict the outlet air conditions with an average difference of 4.93% for the lower manifold, corresponding to an absolute difference of 1.35 °C.

As future lines of work, the influence of fill length and nozzle configuration employed on drift emissions should be studied, although the preliminary results reveal that there are no significant changes with respect to the originals. Another possible line of work would be to modify the channel system to know more precisely the temperature when the arrangement change occurs or modifying the pump to know what happens with lower water-to-air mass flow ratios. In addition, it seems necessary to carry out an analysis with equal nozzles at all levels in order to check if the assumptions made are correct. Finally, another possible objective would be to model the power consumption of the tower, with the aim of checking if the nozzle could be optimised in terms of required pump power consumption and spray characteristics to cover a larger exchange area.

CRediT authorship contribution statement

P. Navarro: Software, Investigation, Formal analysis, Writing – original draft, Writing – review & editing. **J. Ruiz:** Methodology, Software, Formal analysis, Writing – original draft, Writing – review & editing, Funding acquisition. **A.S. Kaiser:** Conceptualization, Writing – review & editing, Supervision, Funding acquisition. **M. Lucas:** Conceptualization, Writing – review & editing, Supervision, Funding acquisition.

Declaration of competing interest

The authors declare that they have no known competing financial interests or personal relationships that could have appeared to influence the work reported in this paper.

Data availability

Data will be made available on request.

Acknowledgements

The authors express their gratitude for the financial assistance received from the Spanish Government and the Government of Valencia (Generalitat Valenciana) through projects ENE2017-83729-C3-1-R (MINECO/AEI/FEDER, UE) and BEST/2019/051 (Subvenciones para estancias de personal investigador doctor en centros de investigación radicados fuera de la Comunitat Valenciana).

References

[1] S.R. Hanna, J. Pell, Cooling tower environment—1974, Environ. Pollut. (1970) 10 (3) (1976) 237, URL: http://www.sciencedirect.com/science/article/pii/0013932776900574.
[2] J.J. Talbot, A review of potential biological impacts of cooling tower salt drift, Atmos. Environ. (1967) 13 (3) (1979) 395–405, URL: http://www.sciencedirect.com/science/article/pii/0004698179902968.
[3] D. McCune, Effects of airborne saline particles on vegetation in relation to variables of exposure and other factors, Environ. Pollut. 74 (3) (1991) 176–203, URL: http://www.sciencedirect.com/science/article/pii/0269749191900699.
[4] EPA, AP–42. Compilation of Air Pollutant Emission Factors, United States. Environmental Protection Agency. Office of Air Quality Planning and Standards, 1995.
[5] V.A. Mouchtouri, G. Goutziana, J. Kremastinou, C. Hadjichristodoulou, Legionella species colonization in cooling towers: Risk factors and assessment of control measures, Am. J. Infect. Control 38 (1) (2010) 50–55, URL: http://www.sciencedirect.com/science/article/pii/S0196655309006282.
[6] J. Ruiz, P. Navarro, M. Hernández, M. Lucas, A. Kaiser, Thermal performance and emissions analysis of a new cooling tower prototype, Appl. Therm. Eng. (2022) 118065, http://dx.doi.org/10.1016/j.applthermaleng.2022.118065, URL: https://www.sciencedirect.com/science/article/pii/S135943112200031X.
[7] BOE, RD 487/2022. Hygienic-Sanitary Criteria for the Prevention and Control of Legionellosis, Spanish Ministry of Health, 2022.
[8] Australian Government, AS/NZS 3666 Air-handling and Water Systems of Buildings. Part 1: Microbial Control - Design, Installation and Commissioning, Standards Australia, 2011.
[9] M. Lucas, J. Ruiz, P.J. Martínez, A.S. Kaiser, A. Viedma, B. Zamora, Experimental study on the performance of a mechanical cooling tower fitted with different types of water distribution systems and drift eliminators, Appl. Therm. Eng. 50 (1) (2013) 282–292.
[10] A. Mohiuddin, K. Kant, Knowledge base for the systematic design of wet cooling towers. Part I: Selection and tower characteristics, Int. J. Refrig. 19 (1) (1996) 43–51, http://dx.doi.org/10.1016/0140-7007(95)00059-3, URL: https://www.sciencedirect.com/science/article/pii/0140700795000593.
[11] A. Mohiuddin, K. Kant, Knowledge base for the systematic design of wet cooling towers. Part II: Fill and other design parameters, Int. J. Refrig. 19 (1) (1996) 52–60, http://dx.doi.org/10.1016/0140-7007(95)00060-7, URL: https://www.sciencedirect.com/science/article/pii/0140700795000607.
[12] A. Mirabdolah Lavasani, Z. Namdar Baboli, M. Zamanizadeh, M. Zareh, Experimental study on the thermal performance of mechanical cooling tower with rotational splash type packing, Energy Convers. Manage. 87 (2014) 530–538, http://dx.doi.org/10.1016/j.enconman.2014.07.036, URL: https://www.sciencedirect.com/science/article/pii/S0196890414006670.
[13] M. Gao, L. Zhang, N.-n. Wang, Y.-t. Shi, F.-z. Sun, Influence of non-uniform layout fillings on thermal performance for wet cooling tower, Appl. Therm. Eng. 93 (2016) 549–555, http://dx.doi.org/10.1016/j.applthermaleng.2015.09.054, URL: https://www.sciencedirect.com/science/article/pii/S1359431115009746.
[14] Y. Zhou, K. Wang, M. Gao, Z. Dang, S. He, F. Sun, Experimental study on the drag characteristic and thermal performance of non-uniform fillings for wet cooling towers under crosswind conditions, Appl. Therm. Eng. 140 (2018) 398–405, http://dx.doi.org/10.1016/j.applthermaleng.2018.05.071, URL: https://www.sciencedirect.com/science/article/pii/S1359431118309402.
[15] A. Tomás, S. Araujo, M.D. Paes, A.R. Primo, J. Da Costa, A. Ochoa, Experimental analysis of the performance of new alternative materials for cooling tower fill, Appl. Therm. Eng. 144 (2018) 444–456, http://dx.doi.org/10.1016/j.applthermaleng.2018.08.076, URL: https://www.sciencedirect.com/science/article/pii/S1359431118323408.
[16] Z. Zhao, J. Gao, X. Zhu, Q. Qiu, Experimental study of the corrugated structure of film packing on thermal and resistance characteristics of cross-flow cooling tower, Int. Commun. Heat Mass Transfer 141 (2023) 106610, http://dx.doi.org/10.1016/j.icheatmasstransfer.2022.106610, URL: https://www.sciencedirect.com/science/article/pii/S0735193322007321.
[17] K. Singh, R. Das, An experimental and multi-objective optimization study of a forced draft cooling tower with different fills, Energy Convers. Manage. 111 (2016) 417–430, http://dx.doi.org/10.1016/j.enconman.2015.12.080, URL: https://www.sciencedirect.com/science/article/pii/S0196890416000029.
[18] K. Singh, R. Das, Simultaneous optimization of performance parameters and energy consumption in induced draft cooling towers, Chem. Eng. Res. Des. 123 (2017) 1–13, http://dx.doi.org/10.1016/j.cherd.2017.04.031, URL: https://www.sciencedirect.com/science/article/pii/S0263876217302678.
[19] A. Dmitriev, I. Madyshev, V. Kharkov, O. Dmitrieva, V. Zinurov, Experimental investigation of fill pack impact on thermal-hydraulic performance of evaporative cooling tower, Therm. Sci. Eng. Prog. 22 (2021) 100835, http://dx.doi.org/10.1016/j.tsep.2020.100835, URL: https://www.sciencedirect.com/science/article/pii/S2451904920303553.
[20] D. Zhang, Z. Zhang, Q. Han, F. Wu, S. He, M. Gao, Numerical simulation on synergetic optimization of non-equidistant fillings and non-uniform water distribution for wet cooling towers, Int. J. Heat Mass Transfer 179 (2021) 121676, http://dx.doi.org/10.1016/j.ijheatmasstransfer.2021.121676, URL: https://www.sciencedirect.com/science/article/pii/S0017931021007821.
[21] W. Deng, F. Sun, Comparative study on the cooling characteristics of different fill layout patterns on a single air inlet induced draft cooling tower, Energies 14 (19) (2021) http://dx.doi.org/10.3390/en14196303, URL: https://www.mdpi.com/1996-1073/14/19/6303.
[22] M. Lemouari, M. Boumaza, I. Mujtaba, Thermal performances investigation of a wet cooling tower, Appl. Therm. Eng. 27 (5–6) (2007) 902–909, http://dx.doi.org/10.1016/j.applthermaleng.2006.08.014, URL: https://www.sciencedirect.com/science/article/pii/S1359431106003036?via%3Dihub.
[23] M. Lemouari, M. Boumaza, A. Kaabi, Experimental analysis of heat and mass transfer phenomena in a direct contact evaporative cooling tower, Energy Convers. Manage. 50 (6) (2009) 1610–1617, http://dx.doi.org/10.1016/j.enconman.2009.02.002, URL: https://www.sciencedirect.com/science/article/pii/S0196890409000545.
[24] M. Lemouari, M. Boumaza, Experimental investigation of the performance characteristics of a counterflow wet cooling tower, Int. J. Therm. Sci. 49 (10) (2010) 2049–2056, http://dx.doi.org/10.1016/j.ijthermalsci.2010.05.012, URL: https://www.sciencedirect.com/science/article/pii/S1290072910001407.
[25] T. Ning, D. Chong, M. Jia, J. Wang, J. Yan, Experimental investigation on the performance of wet cooling towers with defects in power plants, Appl. Therm. Eng. 78 (2015) 228–235, http://dx.doi.org/10.1016/j.applthermaleng.2014.12.032, URL: https://www.sciencedirect.com/science/article/pii/S1359431114011612.
[26] N. Gilani, A. Doustani Hendijani, R. Shirmohammadi, Developing of a novel water-efficient configuration for shower cooling tower integrated with the liquid desiccant cooling system, Appl. Therm. Eng. 154 (2019) 180–195, http://dx.doi.org/10.1016/j.applthermaleng.2019.03.043, URL: https://www.sciencedirect.com/science/article/pii/S135943111930359X.
[27] A.S. Dhurandhar, A.B. Kanase-Patil, Experimental study on effect of water spray characteristics on performance of cooling tower, E3S Web Conf. (2020).
[28] Z. Yu, C. Sun, J. Fang, L. Zhang, Y. Hu, B. Bao, S. Bu, W. Xu, Y. Ji, Water recovery efficiency improvement using the enhanced structure of the mist eliminator, Process Saf. Environ. Prot. 154 (2021) 433–446, http://dx.doi.org/10.1016/j.psep.2021.08.018, URL: https://www.sciencedirect.com/science/article/pii/S0957582021004444.
[29] P. Navarro, J. Ruiz, M. Hernández, A. Kaiser, M. Lucas, Critical evaluation of the thermal performance analysis of a new cooling tower prototype, Appl. Therm. Eng. 213 (2022) 118719, http://dx.doi.org/10.1016/j.applthermaleng.2022.118719, URL: https://www.sciencedirect.com/science/article/pii/S1359431122006639.
[30] J. Kloppers, D. Kröger, A critical investigation into the heat and mass transfer analysis of counterflow wet-cooling towers, Int. J. Heat Mass Transfer 48 (3) (2005) 765–777.
[31] R.K. Singla, K. Singh, R. Das, Tower characteristics correlation and parameter retrieval in wet-cooling tower with expanded wire mesh packing, Appl. Therm. Eng. 96 (2016) 240–249, http://dx.doi.org/10.1016/j.applthermaleng.2015.11.063, URL: https://www.sciencedirect.com/science/article/pii/S1359431115013095.
[32] K. Singh, R. Das, A feedback model to predict parameters for controlling the performance of a mechanical draft cooling tower, Appl. Therm. Eng. 105 (2016) 519–530, http://dx.doi.org/10.1016/j.applthermaleng.2016.03.030, URL: https://www.sciencedirect.com/science/article/pii/S1359431116303222.
[33] F. Merkel, Verdunstungskühlung, VDI Zeitschriff Deutscher Ingen. Berlin, Alemania (1925) 123–128.
[34] M. Poppe, H. Rögener, Berechnung von rückkühlwerken, VDI wärmeatlas (1991) Mi 1.
[35] E. Rubio-Castro, M. Serna-González, J.M. Ponce-Ortega, M.A. Morales-Cabrera, Optimization of mechanical draft counter flow wet-cooling towers using a rigorous model, Appl. Therm. Eng. 31 (16) (2011) 3615–3628, URL: http://www.sciencedirect.com/science/article/pii/S1359431111003887.
[36] Joint Committee for Guides in Metrology (JCGM), Evaluation of measurement data. Guide to the expression of uncertainty in measurement, 2008.
[37] Ashrae, HVAC systems and equipment, in: Chapter 36 Cooling Towers, 2004.
[38] M. Lucas, P. Martínez, A. Viedma, Experimental study on the thermal performance of a mechanical cooling tower with different drift eliminators, Energy Convers. Manage. 50 (2009) 490–497.
[39] F. Gharagheizi, R. Hayati, S. Fatemi, Experimental study on the performance of mechanical cooling tower with two types of film packing, Energy Convers. Manage. 48 (2007) 277–280.
[40] M.A. Ghazani, A.H. ol Hosseini, M.D. Emami, A comprehensive analysis of a laboratory scale counter flow wet cooling tower using the first and the second laws of thermodynamics, Appl. Therm. Eng. 125 (2017) 1389–1401, URL: http://www.sciencedirect.com/science/article/pii/S1359431116345203.
[41] J. Kloppers, D. Kröger, Refinement of the transfer characteristic correlation of wet-cooling tower fills, Heat Transf. Eng. 26 (4) (2005) 035–041, http://dx.doi.org/10.1080/01457630590916266.